ELSEVIER

Palaeogeography, Palaeoclimatology, Palaeoecology 197 (2003) 199–212

PALAEO

www.elsevier.com/locate/palaeo

Late Quaternary hillslope evolution recorded in eastern South African colluvial badlands

M.L. Clarke[a,*], J.C. Vogel[b], G.A. Botha[c], A.G. Wintle[d]

[a] School of Geography, University of Nottingham, University Park, Nottingham NG7 2RD, UK
[b] Quaternary Dating Research Unit, CSIR, P.O.Box 395, Pretoria 0001, South Africa
[c] Council for Geoscience, P.O.Box 900, Pietermaritzburg 3200, South Africa
[d] Institute of Geography and Earth Sciences, University of Wales, Aberystwyth, Ceredigion SY23 3DB, UK

Received 17 August 2001; accepted 16 April 2003

Abstract

Infrared stimulated luminescence (IRSL) ages have been obtained from a sequence of sandy colluvial deposits in northern KwaZulu–Natal. Comparison of the IRSL ages on sand-sized, potassium-rich feldspars, with radiocarbon dates on A-horizon organic matter from buried palaeosols within the colluvial succession shows good agreement between the dating techniques. When compared with palaeoenvironmental records, the data suggest that the colluvium accumulated during arid stages of the Late Quaternary, whilst pedogenesis repeatedly occurred at intervals of hillslope stability which may reflect periods of greater humidity. Temperature does not seem to have been a forcing factor in the landscape development. Extensive colluviation took place during the arid Last Glacial Maximum, but the occurrence of several palaeosols indicates that it was a time of fluctuating climatic conditions.

Keywords: colluvium; hillslope evolution; radiocarbon dating; luminescence dating

1. Introduction

Hillslopes in parts of Swaziland and the KwaZulu–Natal province of South Africa are extensively blanketed by sandy hillwash sediment. These colluvial mantles are often deeply dissected by gully erosion, creating badland topography that exposes a stratigraphic sequence frequently containing several palaeosols. Hillslope processes in this region have clearly undergone a threshold change from net accretion, with periods of active colluviation and intervening pedogenesis, to widespread badland erosion reported by Price Williams et al. (1982); Watson et al. (1984) and Dardis (1990). These authors discuss the investigation of several exposures, mainly in Swaziland, and suggest that the upper colluvium cover was deposited sporadically between 30 and 12 ka ago, and that widespread colluviation occurred during a semi-arid phase associated with the Last Glacial Maximum (LGM) (Price Williams et al., 1982; Watson et al., 1984). The chronological evidence for this interpretation was based on radiocarbon

* Corresponding author.
E-mail address: michele.clarke@nottingham.ac.uk (M.L. Clarke).

0031-0182/03/$ – see front matter © 2003 Published by Elsevier B.V.
doi:10.1016/S0031-0182(03)00461-9

dates for calcrete nodules which formed post-depositionally within the sequences and which could not constrain individual depositional or pedogenic events. As a result of this limitation, it was also not possible to ascertain whether the palaeosols were related to regional climatic change or to local hydrological conditions. At one of these sites, erosion and reworking of colluvium at an accelerating pace was found to have occurred during the last millennium (Dardis, 1990). A subsequent detailed study of various dongas (gullies) in northern KwaZulu–Natal resulted in the construction of a palaeosol-based stratigraphy across the province (Botha, 1996). A chronostratigraphy for this sequence was established with the aid of radiocarbon and luminescence dating (Botha et al., 1990; 1992; 1994; Wintle et al., 1993; 1995a; Botha and Partridge, 2000). Collectively, the results showed that colluviation started during or shortly after the Last Interglacial and continued intermittently into the Post-Glacial period.

The morphogenesis of hillslopes is governed by local climatic conditions and is the result of sequential periods of geomorphic stability and activity. The accumulation of thick sandy colluvium on lower slopes requires an initial humid period of weathering of bedrock and talus to form thick soils and saprolite on hillslopes, stabilised by dense vegetation. A subsequent shift to more arid conditions, with the related decrease in vegetation cover, would allow sheetwash from rainstorm events to transport weathered debris downslope and deposit it as colluvium on more stable slope positions associated with bedrock steps. Sequential climate fluctuations would build up colluvial mantle containing a stratigraphic record of hillslope evolution and pedogenesis. The conditions required for the active development of dendritic gullies and badlands in the colluvial mantle by headwater incision of gully systems initiated further downslope, may be the development of even greater aridity coupled with high intensity rainfall events.

In their review of geomorphological indicators from the humid and sub-humid tropics, Thomas and Thorp (1995) conclude that widespread colluvial deposits may be indicative of aridity or periods of transitional climate. However, no direct comparison of precipitation and colluviation was presented. Using the detailed palynological records for central East Africa, Bonnefille and Chalié (2000) have reconstructed the changes in rainfall over the past 40 ka in the region. In South Africa, however, the pollen record is still somewhat sketchy and the variations in the singula climate during the Late Quaternary (last 120 ka) is not yet well established. In his latest summaries, Scott (1999, 2000) emphasises that it is difficult to separate the effects of temperature and precipitation on past vegetation records. Taking all the available pollen data together, he arrives at the following reconstruction. After the end of the Last Interglacial significant cooling occurred under both relatively humid and drier conditions. At ca. 70 ka the east coast was apparently more humid. Between 40 and 18 ka BP (uncalibrated radiocarbon dates Before Present, i.e. before AD 1950) temperatures decreased to reach a minimum during the LGM, but the evidence suggests that the LGM itself experienced variations in both temperature and rainfall. During the subsequent Late Glacial the pollen data indicate more humidity, while the early Post-Glacial record shows rapid warming under dry conditions, with high precipitation again in Mid-Holocene times.

In addition to the pollen evidence, there are two relatively long records available in South Africa, one of temperature and one of precipitation. Oxygen isotope data for a speleothem from the Cango Caves (Fig. 1) show that temperature at about 35 ka was some 4°C lower than today. The temperature then steadily decreased to reach peak values at times during the LGM of nearly 7°C below that of today, before ultimately increasing to Holocene levels (Talma and Vogel, 1992). The long record of precipitation was obtained from the Pretoria Saltpan (Tswaing Crater) (Partridge et al., 1993, 1997). It is based on a novel approach that relies upon a correlation between soil sediment texture and present-day precipitation and shows an apparent average trend towards drier conditions since the Last Interglacial, albeit with several large oscillations, the earlier ones of which correlate with the calculated changes in latitudinal insolation.

As identified by Thomas and Thorp (1995), the

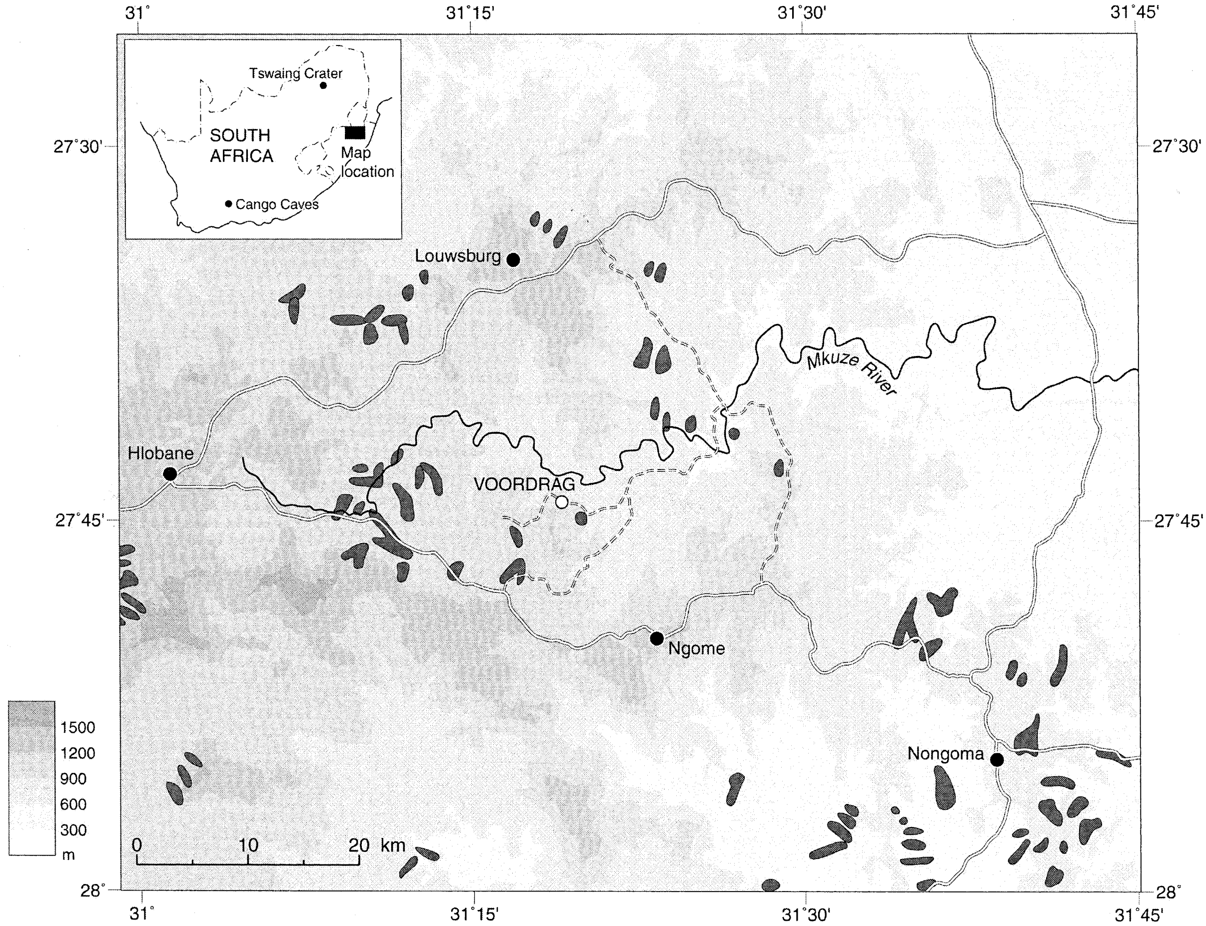

Fig. 1. Map of the study area showing the location of Voordrag, Cango Caves and the Pretoria Saltpan (Tswaing Crater). Identified areas of colluvial deposits are indicated.

timing of successive hillslope events is needed in order to relate hillslope instability to climatic forcing factors. The presence of organic matter in the sequence of buried palaeosols within the colluvial succession enables radiocarbon dating to provide a chronology for periods of hillslope stability, while luminescence dating of the accreted colluvial sediments provides a chronology of instability and geomorphic change. Thus, a combined approach of both radiocarbon and luminescence dating may reveal a detailed record of hillslope evolution. At the same time it can provide evidence for the validity of the specific luminescence technique applied. A gullied colluvial sequence on the farm Voordrag 581 in northern KwaZulu–Natal province with its multiple palaeosol horizons presents an excellent opportunity for investigating both the record of hillslope evolution and the validity of dating using a method based on the IRSL from potassium-rich feldspars.

1.1. Application of luminescence dating

A basic requirement for successful luminescence dating of sediment is that the material be exposed to sunlight for long enough just before burial to remove any pre-existing luminescence signal. The size of the signal that subsequently accumulates over time as the result of exposure to natural sources of ionising radiation in the sediment, provides a measure of the age of the deposit. The challenge in luminescence dating research lies in assessing the efficiency of the initial resetting (zeroing) of the luminescence signal in the mineral grains before deposition. Aeolian transport processes (creep, saltation, reptation and suspension) provide sufficient opportunity for exposure of sediment grains to sunlight to zero the luminescence signal. Infrared stimulated luminescence (IRSL) dating has shown good agreement with independent age control in a number of cases. Agreement with radiocarbon ages was found for aeolian dunes in Oregon (Clarke, 1994), Lapland (Clarke and Käyhkö, 1997), France (Clarke et al., 1999a,b, 2002), and the Great Plains (Clarke and Rendell, 2003). IRSL dating has also been used to provide ages for non-aeolian material, such as fluvial sediments (Fuller et al., 1998), glaciolacustrine silts (Phillips et al., 2000) and alluvial fan sediments (Clarke, 1994; Porat et al., 1996); however, there was no independent age control in these studies. On the other hand, some more recent studies have suggested there is an age underestimation associated with IRSL. For fluvial sediments from the Rhine–Meuse system in The Netherlands, IRSL ages were found to be younger by up to 50% when compared with optically stimulated luminescence (OSL) from quartz (up to 200 ka) and with independent chronology in the last 13 ka (Wallinga et al., 2001). Underestimations of 10–20% compared to radiocarbon dating have also been found for coastal sands from Massachusetts (Van Heteren et al., 2000). Such discrepancies and associated fading results have led Huntley and Lamothe (2001) to conclude that all potassium-rich feldspar ages are underestimated due to signal loss (anomalous fading). They suggest that correction on the basis of laboratory storage experiments carried out over a one-year period are needed. However, Clarke and Rendell (2003) describe IRSL ages for radiocarbon-constrained dunes in Colorado in which the ‘uncorrected’ IRSL ages agree with the bracketing age control and where the ‘corrected’ ages for long-term anomalous fading (following the procedures of Huntley and Lamothe, 2001) are too old. The range of responses found in these published dating studies make it clear that when using IRSL procedures each site must be tested and evaluated on its own merit, and preferably in localities where independent age control exists.

Recent IRSL studies on colluvial sediments in South Africa have involved a limited comparison with radiocarbon dates (Botha et al., 1994; Wintle et al., 1995a,b). At both of the sites investigated there was evidence that the IRSL ages were overestimates. In the present study we apply the single-aliquot additive-dose technique to the IRSL signal from potassium feldspar grains. This approach provides the means of assessing the effectiveness of the pre-depositional zeroing of the luminescence signal (Clarke, 1996). Quartz OSL was not used (Eriksson et al., 1999, 2000), as, at the time the study was carried out, no reliable procedures for correcting for OSL sensitivity changes were available. This site in South Africa, with eleven radiocarbon ages from buried soils, provides a unique opportunity to test for IRSL age underestimation.

2. Site description

The Voordrag site (27°44′30′S, 31°19′30′E) lies in the eastern part of the farm Voordrag 251, 18 km south of the town of Louwsburg (Fig. 1). The extensively eroded colluvial sequence occurs high on the southern valley side of the deeply incised, easterly-draining Mkuze River and on the lower transportational midslope of the Ntumbane Hill to the south. Episodic accretion of sediment occurred within a shallow bowl-shaped depression, incised into siltstone and shales above a thick sandstone unit forming a step on the hillslope as a result of differential stream erosion. Extensive, currently active, badland incision has exposed a composite stratigraphy, up to 18 m thick, of a stacked sequence of colluvial sedimentary units with at least 12 interspersed palaeosols or splits of soil horizons. At no place is more than 11 m of the succession is exposed in any one part of the donga (gully) wall (Figs. 2 and 3). The five palaeosols in the mid-section of the stack comprise very dark grey A and B horizons that contain yellowish–brown iron oxide-coated root channels. The poor development of the soils is reflected in

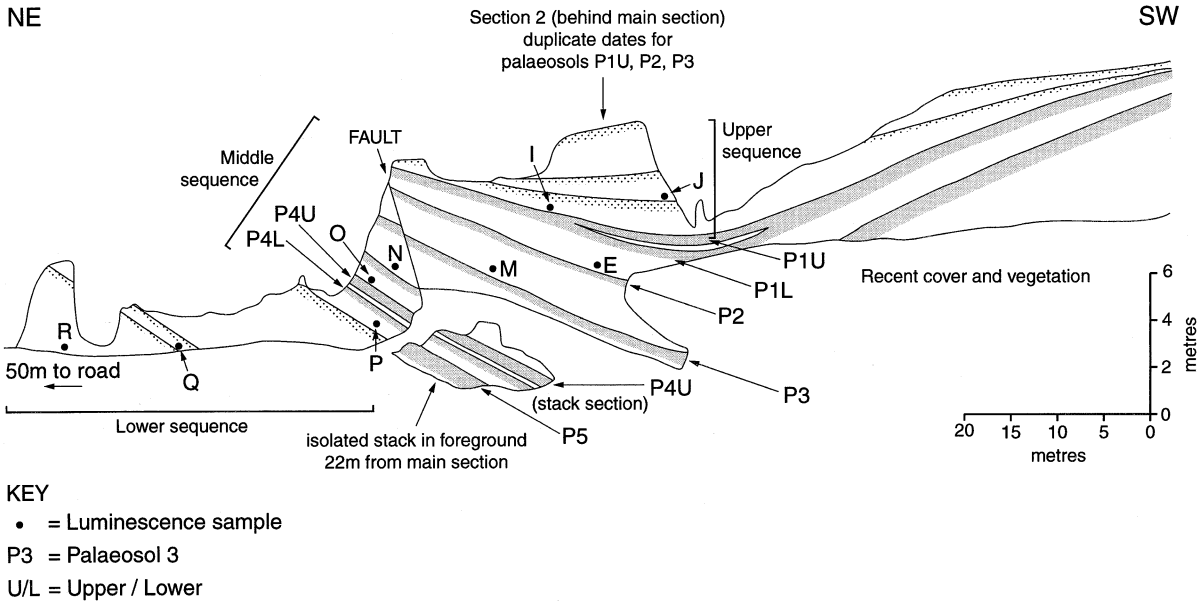

Fig. 2. Cross section of the colluvial succession exposed in the gully wall showing the IRSL sample locations and palaeosols. Note that palaeosol 5 is not found within the main stratigraphic sequence.

the higher clay contents of the A horizons relative to the B horizons, and in organic carbon contents of less than 1% (Botha et al., 1992).

The colluvium was formed by convergence of material transported off a steep sandstone escarpment that forms the northern flank of the Ntumbane Hill. The scarp of the hill is composed of Permian Vryheid Sandstone, which accounts for the sandy nature of the colluvial sediments. Variable sediment accretion in the depression is reflected in changes of the dip of different palaeosol units that suggests differential deposition across the depression as a result of variation in the location of active sediment transport over the hillslope at different times. The basal palaeosols dip at 23° into the depression, while subsequent soil horizons lie at shallower angles as accretion of sediment prograded out from the bedrock face during hillslope evolution. Complete infill of the depression and the current 4° hillslope was only established late in the evolution of this northern slope of Ntumbane Hill. Post-depositional sediment movement within the colluvium-infilled bedrock depression, probably caused by collapse of soil piping or hillslope instability, resulted in minor tensional faults that have displaced some horizons (exposed in the main gully) sidewall locally by several decimetres. The north-facing aspect of the slope will provide maximum solar exposure, which would facilitate the zeroing of the IRSL signal (Porat et al., 2001).

3. Dating of the colluvial sequence

3.1. Radiocarbon dating

The five main buried soil profiles are numbered P1 to P5 from the top down. Palaeosols 1 and 4 have split A horizons (e.g. P1U and P1L), indicating that pedogenesis was briefly interrupted by a pulse of colluvial deposition. The stratigraphic positions of the upper four soils are shown on the schematic profile in Fig. 2. Palaeosol 5 is only represented, together with palaeosol 4, on a separate stack some 20 m away from the main profile. In addition to the five soil samples previously processed (Botha et al., 1992), six new samples were collected in 1993 to obtain a more direct comparison with the IRSL samples. As before,

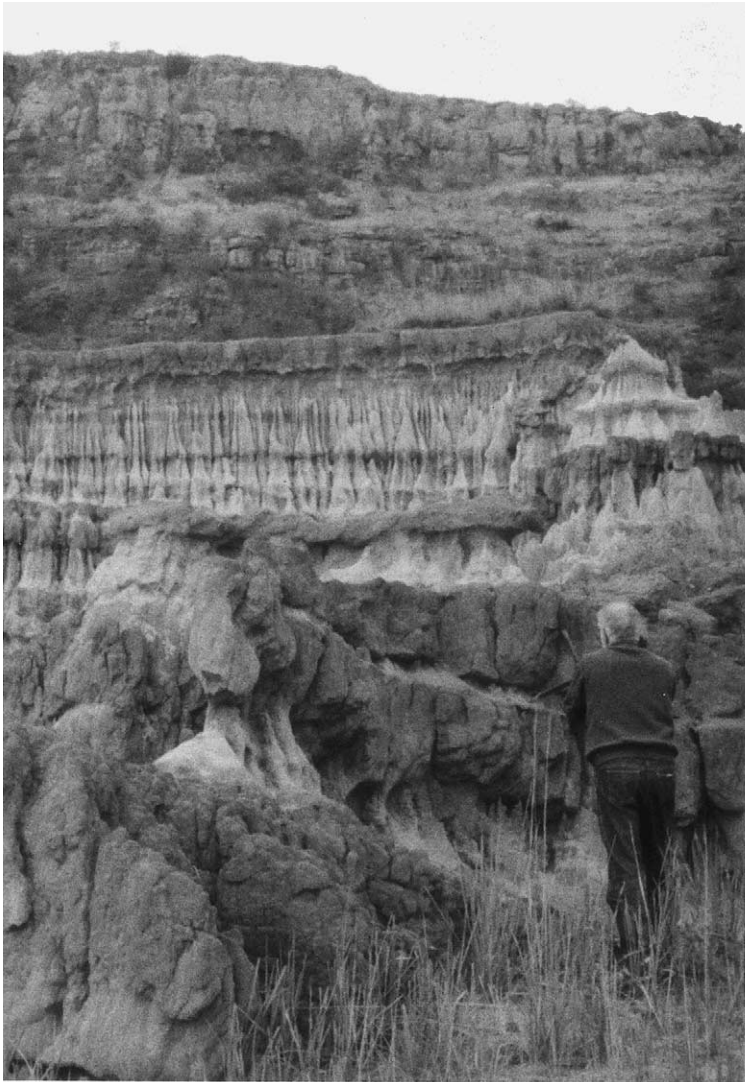

Fig. 3. Photograph of part of the colluvial succession at Voordrag donga.

the material was sieved and the clay and silt fractions (< 20 μm) were used for analysis after removal of the acid solubles. This procedure produces material with a higher concentration of organic matter for analysis. These clay sub-samples contained between 0.6% and 2.9% organic carbon. They were combusted to carbon dioxide, which, after purification, was analysed in proportional radiation counters. The results (Pta-6168 to 6413), together with the previous dates (Pta-5418 to 5440) are given in Table 1.

3.2. Luminescence dating

Nine blocks of colluvial sediment (samples E, I, J, M–R) were taken from a gully side wall (Fig. 2) for luminescence dating. In situ measurement of the γ activity was carried out for all samples (with the exception of sample N) using an NE Technology PSR8 gamma scintillator with a two-inch sodium iodide detector placed at least 30 cm into the face of the exposure. The 180–212-μm potassium feldspar grains (density < 2.58 g/cm^3) were

Table 1
Radiocarbon dates

Laboratory number	Position	C content	$\delta^{13}C$	^{14}C age	Calibrated age
		(%)	(‰)	(years BP)	(ka)
Pta-5429	Palaeosol 1	0.65	−17.4	14500 ± 140	17.3
Pta-6169	Palaeosol 1U	1.7	−17.8	14260 ± 100	17.0
Pta-6173	Palaeosol 1L	1.0	−18.0	17100 ± 170	20.3
Pta-5440	Palaeosol 2	0.85	−16.5	18700 ± 210	22.1
Pta-6170	Palaeosol 2	1.0	−17.0	18600 ± 190	22.0
Pta-5438	Palaeosol 3	1.3	−16.6	19800 ± 220	23.1
Pta-6168	Palaeosol 3	2.9	−14.5	18700 ± 150	22.1
Pta-5420	Palaeosol 4U	2.4	−15.0	34500 ± 810	40.7
Pta-5418	Palaeosol 4L	0.80	−15.2	35700 ± 1000	42.3
Pta-6411	Palaeosol 4U	1.0	−17.8	31200 ± 700	36.8
Pta-6413	Palaeosol 5	1.0	−15.7	37400 ± 1500	43.6

The margin of error of the calibrated dates back to 23.1 ka is ca. 0.3 ka, while the uncertainty of the older dates is considerably larger.

separated using the procedures given in Clarke et al. (1999a,b). The equivalent dose (ED) was determined for 6–18 aliquots per sample, depending upon the quantity of potassium-rich feldspar available. The EDs were derived using the additive-dose procedure of Duller (1994), utilising the dose-correction approach. For non-linear dose response curves, as found for these samples, the additive dose with luminescence correction method is not appropriate, as demonstrated by Duller (1994), and an additional dose correction is required. For two samples with linear growth, Clarke (1994) showed that both correction procedures gave identical results.

Table 2
Single aliquot EDs (Gy) and the fitting errors for individual discs of the different samples

Aliquot number	J	I	E	M	N	O	P	Q	R
1	47.6 ± 3.3	39.4 ± 6.8	63.2 ± 7.8	102 ± 19	89.4 ± 10.1	110 ± 18	181 ± 10	327 ± 15	359 ± 34
2	46.0 ± 2.5	34.3 ± 7.9	57.4 ± 8.4	89.3 ± 3.0	92.3 ± 4.6	93.7 ± 9.0	193 ± 27	295 ± 24	310 ± 21
3	47.0 ± 0.3	37.6 ± 4.1	58.1 ± 5.8	76.0 ± 15	83.0 ± 8.6	97.4 ± 5.3	172 ± 67	341 ± 148	296 ± 12
4	50.8 ± 6.0	30.9 ± 6.7	51.4 ± 7.0	81.8 ± 27	105 ± 0.7	102 ± 13	165 ± 59	355 ± 125	340 ± 26
5	46.6 ± 1.1	38.1 ± 3.7	55.8 ± 2.3	88.7 ± 3.9	96.8 ± 1.8	81.8 ± 20	179 ± 44	312 ± 61	323 ± 16
6	43.4 ± 2.2	34.0 ± 6.0	51.3 ± 4.0	84.8 ± 3.0	82.2 ± 27	105 ± 4.5	178 ± 84	341 ± 156	304 ± 30
7	45.7 ± 9.3	35.4 ± 2.3	65.5 ± 8.9	85.0 ± 11	96.1 ± 4.6	126 ± 60	202 ± 116		
8	44.6 ± 13	36.2 ± 5.1	61.5 ± 2.9	87.2 ± 10	97.5 ± 11	102 ± 4.2	185 ± 38		
9	54.4 ± 8.5	29.4 ± 8.6	59.4 ± 2.6	95.1 ± 1.6	96.6 ± 5.9	101 ± 5.1	181 ± 130		
10	51.0 ± 13	38.8 ± 4.5	60.2 ± 8.4	86.3 ± 4.6	97.6 ± 9.2	100 ± 1.9	167 ± 60		
11	39.8 ± 11	41.5 ± 3.3	55.7 ± 8.1	83.7 ± 5.5	102 ± 4.7	103 ± 7.7	197 ± 11		
12	43.6 ± 4.6	36.9 ± 5.6	49.9 ± 5.4	80.4 ± 11	88.5 ± 2.1	92.9 ± 8.5	167 ± 51		
13		37.5 ± 4.1	57.0 ± 5.3	113 ± 30	104 ± 29	94.8 ± 1.1			
14		37.7 ± 2.7	49.3 ± 1.3	85.9 ± 4.7	104 ± 35	92.1 ± 7.3			
15		41.4 ± 4.3	50.4 ± 1.9	79.6 ± 1.3	91.8 ± 6.2	91.5 ± 7.8			
16		43.1 ± 4.8	52.3 ± 1.0	77.5 ± 3.7	88.0 ± 3.4	89.3 ± 6.1			
17		38.4 ± 4.9	42.9 ± 5.9	71.1 ± 26		86.4 ± 7.6			
18		39.6 ± 2.7	50.9 ± 3.8	83.4 ± 3.4					
χ	46.7	37.2	55.1	86.1	94.7	98.3	181	329	322
σ_{n-1}	3.9	3.5	5.7	9.6	7.2	10	12	22	24
S_N	0.084	0.095	0.104	0.112	0.076	0.104	0.067	0.067	0.074

Table 3
Unattenuated dosimetry measurements and field γ activity

Sample	α count rate (cts/ks cm^{-2})	U (μg/g)	Th (μg/g)	Dry infinite β activity (Gy/ka)	Internal K (%)	Field γ activity (Gy/ka)
J	0.502 ± 0.009	2.33 ± 0.25	6.36 ± 0.81	2.95 ± 0.05	12.03	1.50 ± 0.03
I	0.447 ± 0.006	1.82 ± 0.20	6.52 ± 0.64	2.90 ± 0.10	11.28	1.50 ± 0.03
E	0.296 ± 0.005	1.00 ± 0.17	5.02 ± 0.55	2.56 ± 0.06	11.10	1.71 ± 0.02
M	0.721 ± 0.012	2.34 ± 0.39	12.51 ± 1.28	3.07 ± 0.17	11.10	2.00 ± 0.01
N	0.532 ± 0.009	2.27 ± 0.27	7.43 ± 0.87	2.72 ± 0.09	11.60	–
O	0.399 ± 0.006	1.75 ± 0.18	5.39 ± 0.59	2.69 ± 0.09	11.08	1.58 ± 0.01
P	0.522 ± 0.009	2.00 ± 0.28	8.04 ± 0.99	2.50 ± 0.07	11.68	1.77 ± 0.02
Q	0.461 ± 0.009	2.15 ± 0.24	5.79 ± 0.78	2.74 ± 0.08	11.74	1.84 ± 0.01
R	0.591 ± 0.011	3.12 ± 0.29	6.21 ± 0.94	2.66 ± 0.07	11.91	1.76 ± 0.01

The individual ED values obtained after dose and preheat correction are given in Table 2. These multiple ED determinations enable application of a test for samples that may have been poorly bleached at deposition (Li, 1994; Clarke, 1996); this test involves the nature of the relationship between ED and natural luminescence intensity. Tests for anomalous fading were undertaken on four aliquots of each sample by adding a β dose equivalent to the mean ED for that sample, preheating as above and recording the response to a 0.1-sec infrared (IR) exposure. The aliquots were then stored in the dark and the responses to further IR exposures measured at monthly intervals. No anomalous fading was found in any sample after a storage period of 1 year.

Laboratory measurements of the radioactivity of the sediments were carried out as described by Clarke et al. (1999a,b) and the data obtained are presented in Table 3. The attenuated dosimetry data are shown in Table 4, where the dose rate data have been corrected for grain size and moisture content. The measured moisture contents of the colluvial samples were less than 1% dry weight. However, colluvium accretion occurred in a bowl-shaped depression that would have been wetter than today. The presence of wetland flora pollen, coupled with ferruginous plinthic mottling and iron-stained root channels, indicates that the colluvium experienced accretion and subsequent pedogenesis in a poorly drained environment subject to fluctuating vadose zone conditions (Botha et al., 1992). The evolution of the colluvial fill suggests that the deposits will have been wet throughout sediment accretion within the hollow and the current dryness would only have affected sub-surface moisture contents after gully incision. The γ dose measured in the field was thus attenuated for the presence of considerably more water (i.e. 30 ± 5% wet weight).

Table 4
Attenuated dose rates, ED and IRSL ages

Sample	Internal β dose rate (mGy/a)	External α dose rate (mGy/a)	External β dose rate (mGy/a)	External γ dose rate (mGy/a)	Cosmic dose rate (mGy/a)	Total dose rate (mGy/a)	ED (Gy)	Age (a)
J	656 ± 81	165 ± 90	1744 ± 147	889 ± 112	146 ± 15	3595 ± 221	46.7 ± 3.9	12990 ± 1350
I	611 ± 76	149 ± 77	1711 ± 152	859 ± 109	133 ± 13	3463 ± 217	37.2 ± 3.5	10750 ± 1220
E	601 ± 75	99 ± 52	1507 ± 129	707 ± 89	116 ± 12	3030 ± 182	55.1 ± 5.7	18190 ± 2190
M	601 ± 75	241 ± 125	1811 ± 181	1092 ± 138	110 ± 11	3855 ± 270	86.1 ± 9.6	22330 ± 2930
N	628 ± 78	177 ± 92	1606 ± 143	871 ± 110	105 ± 11	3387 ± 217	94.7 ± 7.2	27950 ± 2780
O	600 ± 70	132 ± 69	1589 ± 142	781 ± 99	99 ± 10	3201 ± 199	98.3 ± 10	30690 ± 3720
P	632 ± 79	174 ± 91	1476 ± 129	832 ± 105	88 ± 9	3202 ± 206	181 ± 12	56460 ± 5210
Q	636 ± 79	153 ± 79	1618 ± 141	821 ± 104	85 ± 9	3313 ± 208	329 ± 22	99220 ± 9080
R	645 ± 80	195 ± 102	1567 ± 135	861 ± 109	85 ± 9	3353 ± 217	322 ± 24	95990 ± 9480

4. Results

4.1. Radiocarbon dating

The new set of radiocarbon ages (Pta-6168 to 6413) confirms the previous set (Pta-5418 to 5440), despite the fact that the samples were collected from different places in the profile (see Fig. 2). This suggests that contamination with younger organic substances was not a serious problem for most of the samples. The sample from the upper part of Palaeosol 4 (P4U) in the isolated stack (Pta-6411) is, however, somewhat younger than its counterpart from the main profile (Pta-5420). This may have been caused by humus infiltration from the immediately overlying grass cover on the surface of the stack. Assuming the difference to be due to contamination and that the sample from Palaeosol 5 in the stack contains the same amount of contamination, the actual age of the soil will become ca. 48 000. This date must, however, be considered a minimum age.

The use of an organic fraction for dating palaeosols is problematic because younger humic substances can often be introduced by percolating soil moisture from higher up the deposit. This is demonstrated from radiocarbon dating of the Paudorf soil at Gottweig–Aigen in Austria where a charcoal sample produced an age of 32.1 ka, while two samples of humus extract from the same level gave 27.7 and 22.7 ka (Vogel and Zagwijn, 1967). That this is not invariably the case is shown by two dates for the Paudorf soil at Dolni Vestonice in the Czech Republic where charcoal gave 29.0 ka and the humus 28.3 ka (Vogel and Zagwijn, 1967). Provided local conditions do not favour downward penetration of humic material, and sufficient care is taken to remove the mobile fulvic acids from the sample, it is possible to obtain reliable dates. The effect of younger contamination on the apparent age becomes greater the older the palaeosol is, while it is only a relatively young contaminant that has a serious affect on the result. The situation at the Voordrag site was considered favourable for the dating of the palaeosols since they occur at a considerable depth below the original surface and the transmissivity of the deposit is not great. This however, does not apply to two of the oldest soils sampled from an isolated stack which has remnants of the recent soil coverage less than a metre above.

For comparison with the IRSL dates, the radiocarbon ages need to be calibrated to calendar dates. This is done using the Pretoria Calibration Program that is based on the INTCAL98 data (Stuiver et al., 1998) adjusted for the Southern Hemisphere for the period younger than 24 ka, and on the curve produced by Vogel and Kronfeld (1997) for the older period.

4.2. Luminescence dating

As discussed by Clarke et al. (1999a,b), it is possible to assess the efficiency of solar resetting at burial. This can be achieved by evaluating the variation in the recorded EDs of the individual aliquots (Table 2) and by consideration of normalised plots of ED vs. natural IRSL intensity for the individual aliquots. Three such plots are shown in Fig. 4, two from Voordrag (samples I and N) and one for a sample from a colluvial deposit at St Paul's, elsewhere in KwaZulu–Natal (Wintle et al., 1995a). A sample of uniform composition that had its IRSL zeroed would give a cluster of points around the centre point of the graph as both ED and natural intensity would give almost identical results. In the case of a well-bleached sediment containing grains of different sensitivity, the points would lie along a horizontal line with the normalised EDs clustered around 1.00. Both of these types of behaviour have been shown to exist in aeolian dune sand (Clarke, 1996). Fig. 4 shows that for samples I and N from Voordrag, the values of ED are clustered, compared with the sample from St Paul's, which was considered poorly bleached (Li, 1994).

In Table 2 the individual single aliquot EDs obtained for each sample are presented, along with the mean ED (χ), the standard deviation on the mean (σ_{n-1}) and the relative error (or coefficient of variation), S_N given as $(\sigma_{n-1})/\chi$ using the notation of Clarke (1996). Based on her experimental study, she proposed criteria for detecting samples that contained poorly bleached grains. Specifically, samples with values of S_N that are >0.10 indicate the presence of poorly

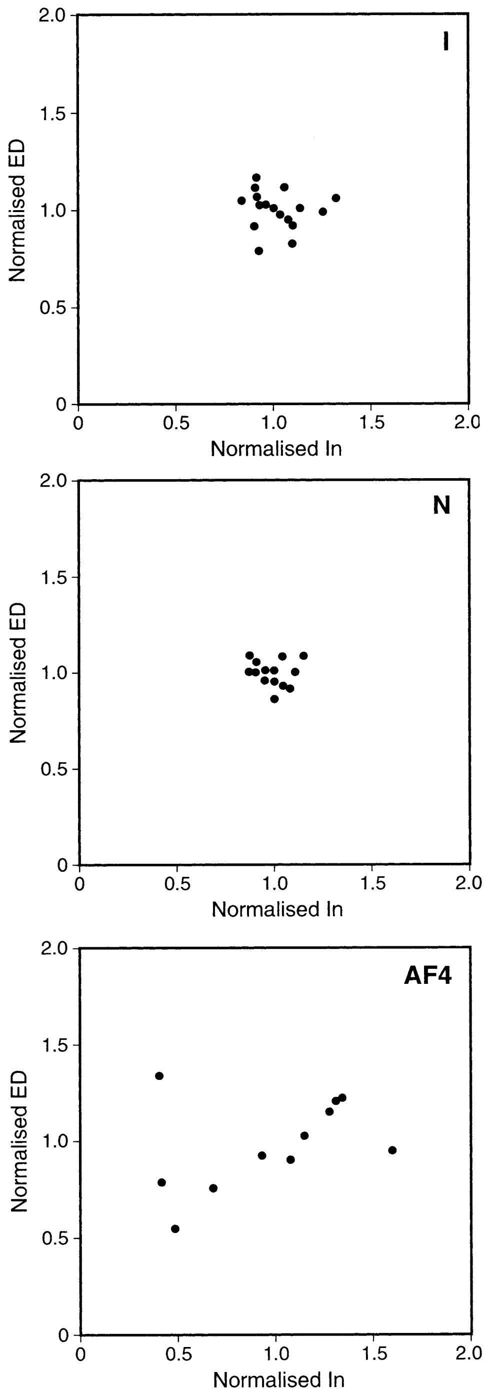

Fig. 4. Normalised scatter plots of ED against natural IRSL intensity for two samples from Voordrag (I and N) and for one from St Paul's (AF4) with data from Li (1994).

bleached grains. In Table 2, the values of S_N are less than 0.10 (i.e. have a relative error of < 10%), apart from samples E, M and O, for which the samples are only slightly over the limit with S_N of 0.104, 0.111 and 0.104, respectively. Thus, the samples in this study can be taken to have been sufficiently bleached at deposition to permit the calculation of reliable ages from the mean ED and error given in Table 2. These values were used to calculate the ages in Table 4.

5. Discussion

5.1. The chronology

The IRSL ages show a highly satisfactory agreement with the calibrated radiocarbon dates (Fig. 5). This shows that single aliquot IRSL can give accurate ages for the Late Pleistocene, once it has been demonstrated that the grains were initially adequately zeroed. The one exception is the date of 43.6 ka for Palaeosol 5 and the IRSL age of 56.5 ka for the colluvium immediately above it. As discussed above, this might be the result of a small amount of modern carbon contamination in the isolated stack. A corrected age of 48 ka would produce a calibrated age of ca. 50 ka, which is well within the error limit of the IRSL age, but must also be taken as a minimum age.

The stratigraphic sequence, revealed by the badland gully incision, is one of apparent episodic colluvial deposition with intervening periods of stability and pedogenesis. There is no evidence of repetitive palaeogully erosion at Voordrag, although some episodes of cut and fill are recorded in the stratigraphy elsewhere in KwaZulu–Natal (Botha et al., 1994). For the sake of clarity and subsequent comparison with local palaeoclimatic data, the sequence will be discussed in terms of the marine oxygen isotope stages (OIS). The results show that deposition of the dated colluvial succession commenced at the end of the Last Interglacial (OIS 5e), between 90 and 100 ka ago (samples Q and R; Figs. 2 and 5). This timing for the start of colluvial deposition has also been found at other sites in the province (Wintle et al., 1995a). The lack of any older col-

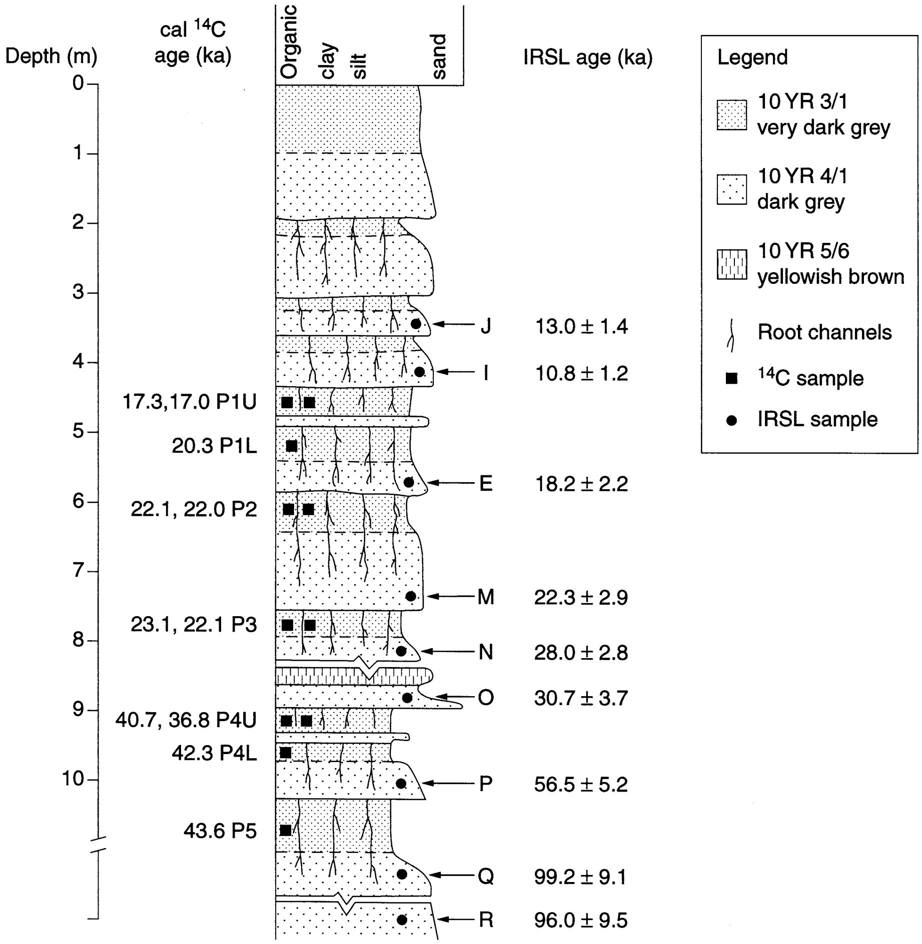

Fig. 5. Composite stratigraphy of the succession at Voordrag showing the IRSL and calibrated radiocarbon dates (Pta analysis numbers beginning with 5 are taken from Botha et al., 1992). See Table 1 and the text for the error margins of the ^{14}C dates.

luvium suggests that during the preceding Interglacial (OIS 5e), the hillslopes were largely stripped of their older colluvial mantle. A period of intense weathering on the uphill slopes followed, to produce material that would be available for transport downslope later in OIS 5. Above sample Q colluviation dominated the landscape (Fig. 2) until stability set in and the relatively massive soil, P5, developed.

During OIS 2, the LGM, accumulation of colluvium in the hollow increased to produce the main sedimentary sequence at the site. The colluviation was interspersed with four brief periods of pedogenesis (P1 upper, P1 lower, P2, and P3). This phase continued to the end of OIS 2 (samples J and I). It was followed by further episodic accretion through the earlier part of the Post-Glacial Holocene, interspersed with thin, weakly pedogenic horizons, until deposition eventually ceased and a well developed soil profile formed on top of the deposit. Finally, this phase of landscape stability was replaced by the intense badland erosion and colluvial dissection that is still ongoing today.

The overall conclusion that can be drawn from these dates is that colluviation at the site started during the early stages of the Last Glacial (late OIS 5) and continued with increasing intensity throughout the period with several interruptions during which soil profiles developed, until well into the Post-Glacial. The land-surface fluctuations between deposition and pedogenesis over the past 100 000 years indicate that the hillslope response was close to the geomorphic threshold between activity and stability. This was especially the case during the LGM.

5.2. The palaeoenvironmental record

Given the chronological control established through both radiocarbon dating of the palaeosols and IRSL dating of the colluvium, it is possible to compare the record with the available climatic data. It is obvious that temperature was not a controlling factor for either colluvium accretion or soil formation, since both occurred, for instance, during the cold LGM and the warm Early Holocene as recorded in the Cango Cave temperature records (Talma and Vogel, 1992). The Voordrag sequence does, however, appear to reflect changes in regional precipitation, which also may reflect enhanced seasonality. When compared with the rainfall record for the Tswaing Crater (Fig. 6), it is noted that the driest recorded period, which dates to the LGM, corresponds to the substantial 3 m accumulation of colluvium at Voordrag. The underlying unit dated to 56.5 ± 5.2 ka (sample P) may coincide with the dry phase at 61 ka at Tswaing and the basal accumulation before that, dated to 99.2 and 96.0 ka (samples Q and R), could have occurred during the dry oscillation at 104 ka. The considerable package of colluvia between these two events (see Fig. 2) may correspond to the dry phase shown at 80 ka. On the other hand, there is no indication of colluvium during the dry event at 44 ka. The upper part of the Tswaing section, for which actual radiocarbon dates exist, does not reflect the palynologically identified humid periods on both sides of the Early Holocene warm, dry phase, but shows continuous aridity between 25 and 3 ka (Fig. 6). However, the pollen evidence elsewhere does seem to be reflected in the upper 4 m of colluvium at Voordrag (Fig. 5). This was deposited between the Late Glacial palaeosol, P1, and the substantial soil horizon that developed on top of the sequence before erosion set in.

The palaeosols that formed during periods of stability on the hillslope thus seem to represent episodes of sustained humidity within the sequence of hillslope genesis. Specifically, the soils that developed during the LGM, confirm Scott's (2000) conclusion that fluctuating conditions prevailed at the time, leading to contradictory indications in the pollen spectra from different sites. Finally it must be pointed out that it is not clear which climatic conditions were responsible for the most recent erosional phase that has created badland topography. What is seen today appears to be a repetition of the situation that occurred towards the end of the previous warm phase of the Last Interglacial (OIS 5e), i.e. removal of the colluvial deposits by gullying.

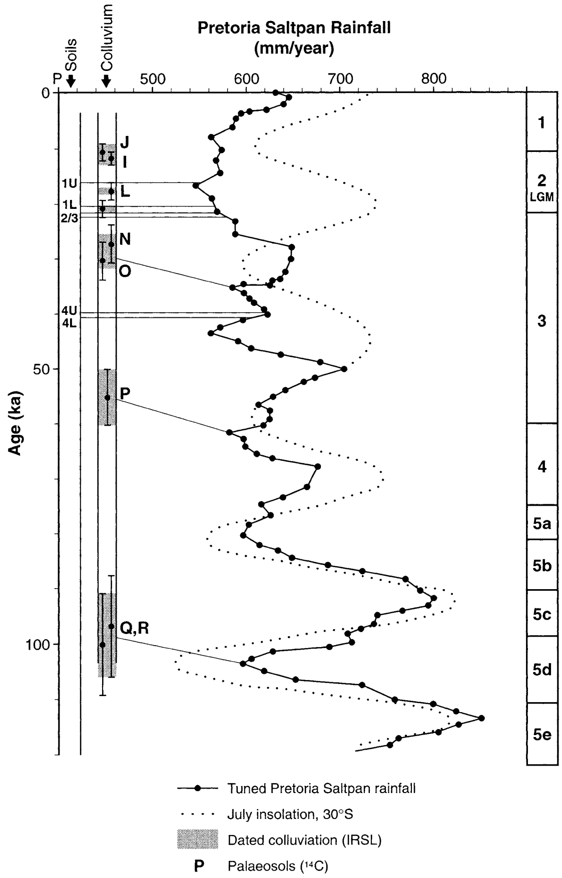

Fig. 6. Rainfall record from Tswaing Crater (Partridge et al., 1997) together with the record of palaeosols and colluvium at Voordrag. P5 is not shown due to the uncertainty associated with its age.

6. Conclusions

The intercalated soils and colluvial units at Voordrag permitted an unusually detailed and direct comparison of the radiocarbon and IRSL dating methods over the last 40 ka. The feldspar grains in all nine samples of colluvium were demonstrated to have been sufficiently light exposed at deposition to inspire confidence in the IRSL dates. The use of the fine fraction in the palaeosols in order to concentrate the organic matter for radiocarbon dating proved effective, and there was no evidence of humic contamination in the deeply buried horizons. The concordance of the radiocarbon and IRSL ages is one of the best demonstrations of the validity of using IRSL for dating colluvial deposits.

Colluviation started at about 100 ka and continued through OIS 4 and 2 with soils formed on several occasions throughout the period from 100 to 10 ka. A comparison of the dates for the soils and colluvium with the precipitation record of the Tswaing Crater suggests that colluvium is formed when the climate in southern Africa is most arid. In contrast, the periods of hillslope stability, represented by the palaeosols P5 and P4, may be related to periods of higher precipitation and vegetation cover in late OIS 4 and in OIS 3. During OIS 2, the generally greater aridity led to higher rates of colluvial accumulation, but the development of palaeosols (P1, P2 and P3) at this time suggests climatic fluctuation during the LGM.

Acknowledgements

The IRSL research was funded by NERC grant GR9/644A and the results were first presented at the 9th International Conference of Luminescence and Electron Spin Resonance Dating held in Canberra, Australia, in 1996.

References

Bonnefille, R., Chalié, F., 2000. Pollen-inferred precipitation time-series from equatorial mountains, Africa, the last 40 kyr BP. Glob. Planet. Change 26, 25–50.

Botha, G.A., 1996. The Geology and Palaeopedology of Late Quaternary Colluvial Sediments in Northern KwaZulu/Natal. Counc. Geosci. Mem. 83, 165 pp.

Botha, G.A., de Villiers, J.M., Vogel, J.C., 1990. Cyclicity of erosion, colluvial sedimentation and palaeosols formation in Quaternary hillslope deposits from northern Natal, South Africa. Palaeoecol. Afr. 21, 195–210.

Botha, G.A., Scott, L., Vogel, J.C., von Brunn, V., 1992. Palaeosols and palaeoenvironments during the Late Pleistocene Hypothermal in northern Natal. S. Afr. J. Sci. 88, 508–512.

Botha, G.A., Wintle, A.G., Vogel, J.C., 1994. Episodic Late Quaternary palaeogully erosion in northern KwaZulu–Natal, South Africa. Catena 23, 327–340.

Botha, G.A., Partridge, T.C., 2000. Colluvial deposits. In: Partridge, T.C., Maud, R.R. (Eds.), The Cenozoic of Southern Africa. Oxford University Press, Oxford, pp. 88–99.

Clarke, M.L., 1994. Infra-red stimulated luminescence ages from aeolian sand and alluvial fan deposits from the Eastern Mojave Desert, California. Quat. Geochron. (Quat. Sci. Rev.) 13, 533–538.

Clarke, M.L., 1996. IRSL dating of sands: Bleaching characteristics at deposition inferred from the use of single aliquots. Radiat. Meas. 26, 611–620.

Clarke, M.L., Käyhkö, J.A., 1997. Evidence of Holocene aeolian activity in sand dunes from Lapland. Quat. Geochron. (Quat. Sci. Rev.) 16, 341–348.

Clarke, M.L., Rendell, H.M., 2003. Late Holocene dune accretion and episodes of persistent drought in the Great Plains of northeastern Colorado. Quat. Sci. Rev. 22, 1051–1058.

Clarke, M.L., Rendell, H.M., Pye, K., Tastet, J.-P., Pontee, N.I., Massé, L., 1999a. Evidence for the timing of dune development on the Aquitaine Coast, southwest France. Z. Geomorphol. Suppl. 116, 147–163.

Clarke, M.L., Rendell, H.M., Tastet, J.-P., Clavé, B., Massé, L., 2002. Late Holocene sand invasion and North Atlantic storminess along the Aquitaine Coast, southwest France. Holocene 12, 231–238.

Clarke, M.L., Rendell, H.M., Wintle, A.G., 1999b. Quality assurance in luminescence dating. Geomorphology 29, 173–185.

Dardis, G.F., 1990. Late Holocene erosion and colluvium deposition in Swaziland. Geology 18, 934–937.

Duller, G.A.T., 1994. Luminescence dating using single aliquots: New procedures. Quat. Geochron. (Quat. Sci. Rev.) 13, 149–156.

Eriksson, M.G., Olley, J.M., Payton, R.W., 1999. Late Pleistocene colluvial deposits in central Tanzania: Erosional response to climatic change? GFF 121, 198–201.

Eriksson, M.G., Olley, J.M., Payton, R.W., 2000. Soil erosion history in central Tanzania based on OSL dating of colluvial and alluvial hillslope deposits. Geomorphology 36, 107–128.

Fuller, I.C., Macklin, M.G., Lewin, J., Passmore, D.G., Wintle, A.G., 1998. River response to high-frequency climate oscillations in southern Europe over the last 200 k.y.. Geology 26, 275–278.

Huntley, D.J., Lamothe, M., 2001. Ubiquity of anomalous fading in K-feldspars and the measurement and correction for it in optical dating. Can. J. Earth Sci. 38, 1093–1106.

Li, S.-H., 1994. Optical dating: Insufficiently bleached sediments. Radiat. Meas. 23, 563–567.

Partridge, T.C., Kerr, S.J., Metcalfe, S.E., Scott, L., Vogel, J.C., 1993. The Pretoria Saltpan: A 200,000 year South African lacustrine sequence. Palaeogeogr. Palaeoclimatol. Palaeoecol. 101, 317–337.

Partridge, T.C., Demenocal, P.B., Lorentz, S.A., Paiker, M.J., Vogel, J.C., 1997. Orbital forcing of climate over South Africa: A 200,000-year rainfall record from the Pretoria Saltpan. Quat. Sci. Rev. 16, 1125–1133.

Phillips, W.M., Sloan, V.F., Shroder, J.F., Jr., Sharma, P., Clarke, M.L., Rendell, H.M., 2000. Asynchronous glaciation at Nanga Parbat, northwestern Himalaya Mountains, Pakistan. Geology 28, 431–434.

Porat, N., Wintle, A.G., Amit, R., Enzel, Y., 1996. Late Quaternary earthquake chronology from luminescence dating of colluvial and alluvial deposits of the Arava valley, Israel. Quat. Res. 46, 107–117.

Porat, N., Zilbermann, E., Amit, R., Enzel, Y., 2001. Residual ages of modern sediments in an hyperarid region, Israel. Quat. Sci. Rev. 20, 795–798.

Price Williams, D., Watson, A., Goudie, A.S., 1982. Quaternary colluvial stratigraphy, archaeological sequences and palaeoenvironment in Swaziland, southern Africa. Geogr. J. 148, 50–67.

Scott, L., 1999. Vegetation history and climate in the Savanna biome South Africa since 190,000 ka: A comparison of pollen data from the Tswaing Crater (the Pretoria Saltpan) and Wonderkrater. Quat. Int. 57/58, 215–223.

Scott, L., 2000. Pollen. In: Partridge, T.C., Maud, R.R. (Eds.), The Cenozoic of Southern Africa. Oxford University Press, Oxford, pp. 339–350.

Stuiver, M., Reimer, P.J., Bard, E., Beck, J.W., Burr, G.S., Hughen, K.A., Kromer, B., McCormac, G., Van der Plicht, J., Spurk, M., 1998. INTCAL98 radiocarbon age calibration, 24,000–0 cal BP. Radiocarbon 40, 1041–1083.

Talma, A.S., Vogel, J.C., 1992. Late Quaternary palaeotemperatures derived from a speleothem from Cango Caves, Cape Province, South Africa. Quat. Res. 37, 203–213.

Thomas, M.F., Thorp, M.B., 1995. Geomorphic response to rapid climatic and hydrologic change during the Late Pleistocene and Early Holocene in the humid and sub-humid tropics. Quat. Sci. Rev. 14, 193–207.

Van Heteren, S., Huntley, D.J., van de Plassche, O., Lubberts, R.K., 2000. Optical dating of dune sand for the study of sea level change. Geology 28, 411–414.

Vogel, J.C., Kronfeld, J., 1997. Calibration of radiocarbon dates for the Late Pleistocene using U/Th dates on stalagmites. Radiocarbon 39, 27–232.

Vogel, J.C., Zagwijn, W.H., 1967. Radiocarbon dates VI. Radiocarbon 9, 63–106.

Wallinga, J., Murray, A.S., Duller, G.A.T., Tornqvist, T.E., 2001. Testing optically stimulated luminescence dating of sand-sized quartz and feldspar from fluvial deposits. Earth Planet. Sci. Lett. 193, 617–630.

Watson, A., Price Williams, D., Goudie, A.S., 1984. The palaeoenvironmental interpretation of colluvial sediments and palaeosols of the Late Pleistocene Hypothermal in southern Africa. Palaeogeogr. Palaeoclimatol. Palaeoecol. 45, 225–249.

Wintle, A.G., Li, S.-H., Botha, G.A., 1993. Luminescence dating of colluvial deposits from Natal, South Africa. S. Afr. J. Sci. 89, 77–82.

Wintle, A.G., Botha, G.A., Li, S.-H., Vogel, J.C., 1995a. A chronological framework for colluviation during the last 110 kyr in KwaZulu/Natal. S. Afr. J. Sci. 91, 134–139.

Wintle, A.G., Li, S.-H., Botha, G.A., Vogel, J.C., 1995b. Evaluation of luminescence dating procedures applied to late-Holocene colluvium near St Paul's Mission, Natal, South Africa. Holocene 5, 97–102.